Proc. XIVth Int. Congr. on Rheology
Edited by:

August 22-27, 2004
Seoul, Korea

Visualizations of viscoelastic flow in a 4:1 square/square contraction

Manuel A. Alves[a], Fernando T. Pinho[b], Paulo J. Oliveira[c]

[a]Dep. Eng. Química, CEFT, Faculdade Engenharia Universidade Porto, 4200-465 Porto, Portugal
[b]Centro de Estudos de Fenómenos de Transporte, DEM, Univ. Minho, 4800-058 Guimarães, Portugal
[c]Dep. Eng. Electromecânica, Unidade MTP, Univ. Beira Interior, 6201-001 Covilhã, Portugal

ABSTRACT

Visualizations of the 3D-flow in a 4:1 square-square sudden contraction were carried out with a Newtonian fluid, a Boger fluid and a shear-thinning viscoelastic fluid under conditions of negligible inertia. Whereas for the Newtonian fluid the vortex remained unchanged with increasing flowrate, vortex enhancement was observed with the viscoelastic liquids (polyacrylamide solutions) with stronger activity in the case of the shear-thinning fluid. At high Deborah numbers the flow became periodic and at higher flowrates chaotic. In the steady flow regime the vortices are not closed and the trajectory of the fluid particles interacting with the vortices is reversed by viscoelasticity.

INTRODUCTION

Sudden contractions are classical benchmark problems used in Computational Rheology [1] and have been mainly investigated in the planar and axisymmetric cases; recent experiments in both geometries were carried out by Nigen and Walters [2]. Investigations in square-square contractions are less common but not unknown: Walters and Webster [3] found similarities between the flows through circular and square/square contractions and the experiments of Walters and Rawlinson [4] also confirmed that the differences between the flow of viscoelastic fluids in planar and 13.3:1 square/square contractions had similarities to the differences observed between planar and circular contractions.

Nevertheless, it is clear that much less is known about the flow of viscoelastic fluids in square/square contractions which may be taken as a prototype of 3D flow for numerical simulations, and this work is part of a wider systematic research on this flow.

EXPERIMENTAL RIG

The experimental set-up is shown in Figure 1. It consisted of two square ducts of length 1000 mm and 300 mm having sides of $2H_1$=24 mm and $2H_2$=6 mm, thus defining a 4:1 contraction ratio.

To visualize the flow a 10 mW He-Ne laser light source was employed. The beam passed through a cylindrical lens to generate a sheet of light illuminating highly reflective tracer particles suspended in the fluid. Their trajectories were recorded using long time exposure photography with a conventional camera (Canon EOS 300 with a macro EF100 mm lens).

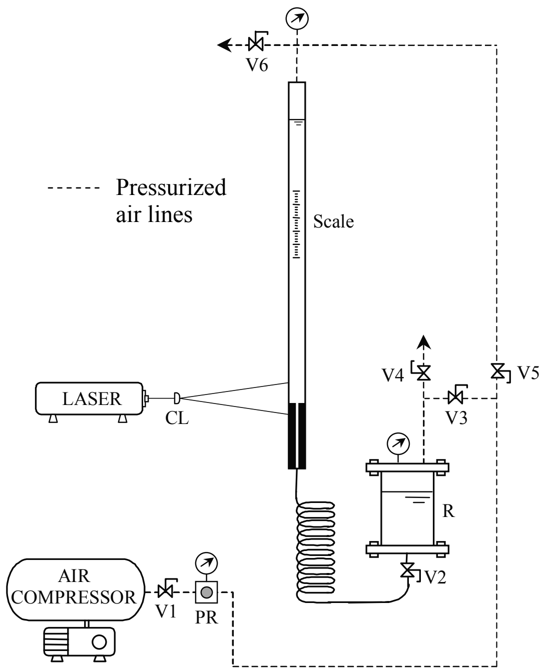

Figure 1. Experimental set-up.

FLUID RHEOLOGY

The shear viscosity (η) and the first normal stress difference coefficient (Ψ_1) in steady shear flow, and the rigidity and loss moduli (G', G'') in oscillatory shear flow were measured with an AR2000 rheometer from TA instruments using a cone-plate geometry. Three fluids were

investigated: a Newtonian fluid (91% glycerin, 7.5% water and 1.5% NaCl), a Boger fluid (100 ppm of polyacrylamide (PAA) in 91% glycerin, 7.5% water and 1.5% NaCl) and a shear-thinning fluid (500 ppm of PAA in 85% glycerin and 15% water). The PAA used in the preparation of the test fluids was Separan AP30 from SNF Floerger, and all concentrations are on a weight basis. A concentration of 25 ppm of a biocide (Kathon LXE produced by Rohm and Haas) was added to all solutions to minimize biological degradation.

The viscosity of the Newtonian fluid (N91) was 0.43 Pa.s at 18°C, the temperature at which the visualizations with this fluid took place. Figures 2 and 3 represent the steady and oscillatory shear properties for the PAA100 and PAA500 fluids, respectively. The data are presented in reduced form; further details are described elsewhere [5].

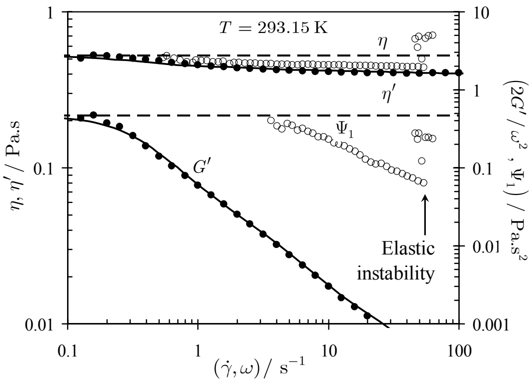

Figure 2. Steady and oscillatory shear properties for PAA100 fluid.

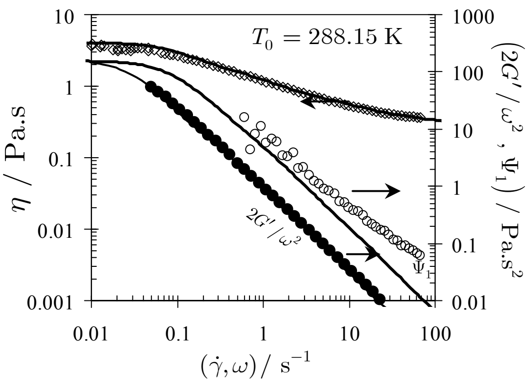

Figure 3. Steady and oscillatory shear properties for PAA500 fluid.

Figures 2 and 3 show the good match between steady and oscillatory shear properties at low deformation rates, the almost constant viscosity of the PAA100 fluid and that PAA500 is moderately shear-thinning, because its viscosity decreases only by a factor of ten between the low and high shear rate plateaux.

Multimode viscoelastic models were fitted to the linear viscoelastic data, to determine the spectra of relaxation times and viscous parameters (λ_k, η_k). From these an equivalent relaxation time $\lambda = \sum \eta_k \lambda_k / \eta_p$ was obtained, with $\eta_p = \sum_{k \neq \text{solvent}} \eta_k$.

The total viscosity at low shear rates, η_0 ($= \eta_s + \eta_p$), and the relaxation time were of 0.52 Pa.s and 1.947 s for the PAA100 solution, and of 4.07 Pa.s and 20.47 s for the PAA500 fluid, respectively.

FLOW VISUALIZATIONS

The flows presented in this section are characterized by Deborah and Reynolds numbers defined on the basis of upstream quantities, as $De = \lambda U_1 / H_1$ and $Re = \rho U_1 H_1 / \eta$.

Figure 4 shows the evolution with the Deborah number of the flow streaklines at the middle plane of the contraction for the Boger fluid (PAA100), which includes the limiting Newtonian case, $De = 0$. For the Newtonian fluid the normalized vortex length is $x_R / H_1 = 0.326$, under negligible inertia flow conditions. Results for the Newtonian fluids, not shown here, show this length to decrease by less than 10% for Reynolds numbers below 0.1 and by less than 5% for $Re < 0.04$.

For the Boger fluid viscous effects predominate at low Deborah numbers ($De = 0.041$) and the flow pattern is similar to that seen for the Newtonian fluid. With increasing elasticity there is a decrease in vortex size to about a quarter at $De \approx 0.2$, an effect not due to inertia since the Reynolds number never exceeded 0.05. Then, as De further increases the corner vortex grows and simultaneously the approach flow streamlines progressively diverge, a typical elastic effect already described by McKinley et al [6] for Boger fluid flows in circular contractions, and predicted by Alves et al [7] for Boger fluid flows in planar contractions. The growth of the large vortex with elasticity continues and eventually the flow becomes periodic at $De \approx 0.8$-0.9 and chaotic at higher flow rates.

The PAA500 solution is both shear-thinning and more elastic than the PAA100 fluid, and this brings in several changes in flow pattern, as can be assessed from inspection of the middle plane streaklines presented in Figure 5. Again inertia is negligible, but the vortex grows significantly and quicker with flow elasticity than for the PAA100 fluid. The initial decrease in vortex length seen for the PAA100, is absent for the PAA500 so that at De = 0.1 it has already duplicated in size

relative to the Newtonian value. At $De = 1$ it has grown sixfold and the flow remains steady at least up to $De = 1.34$. At $De = 1.7$ the flow near the contraction is periodic and at much higher flow rates it becomes eventually chaotic.

A noteworthy feature due to fluid elasticity, clearly observed with the PAA500 solution, not shown here in detail for lack of space, is that the flow direction of fluid particles within the vortices is reversed (see [5,8]). In the steady flow regime the vortices are not closed (cf. Figure 5) and fluid particles enter the middle-plane vortex, rotate towards its eye, drift to the corner plane vortex, then rotate to its periphery and exit to the downstream duct, a dynamic process that is opposite to that found with Newtonian fluids.

ACKNOWLEDGEMENTS

We are grateful for financial support of FEDER via FCT program POCTI/37699/EQU/2001.

REFERENCES

1. Hassager O, J. Non-Newt. Fluid Mech., **29**, 2 (1988).
2. Nigen S and Walters K, J. Non-Newt. Fluid Mech., **102**, 343 (2002).
3. Walters K and Webster MF, Phil. Trans. R. Soc. London A, **308**, 199 (1982).
4. Walters K and Rawlinson DM, Rheol. Acta, **21**, 547 (1982).
5. Alves MA, Laminar flows of viscoelastic fluids: Numerical, theoretical and experimental analysis (in Portuguese). PhD Thesis, Universidade do Porto, Portugal (2004).
6. McKinley GH, Raiford WP, Brown RA, Armstrong RC, J. Fluid Mech., **223**, 411 (1991)
7. Alves MA, Pinho FT and Oliveira PJ, J. Non-Newt. Fluid Mech., **93**, 287 (2000).
8. Alves MA, Pinho FT and Oliveira PJ, Proc. XIVth Int. Congr. on Rheology, Korea (2004).

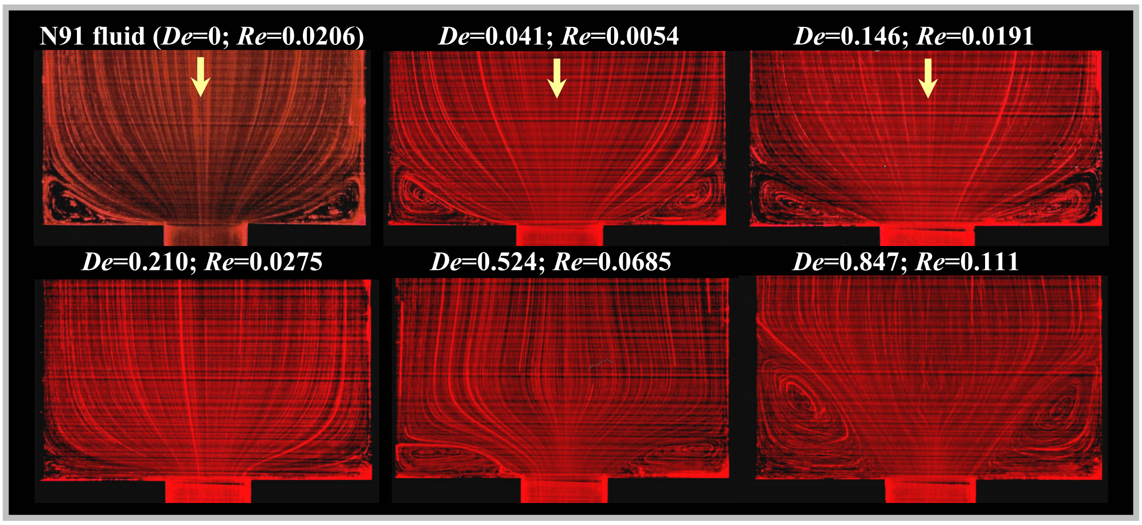

Figure 4. Streaklines in the middle plane as a function of Deborah number for the Newtonian and PAA100 fluid.

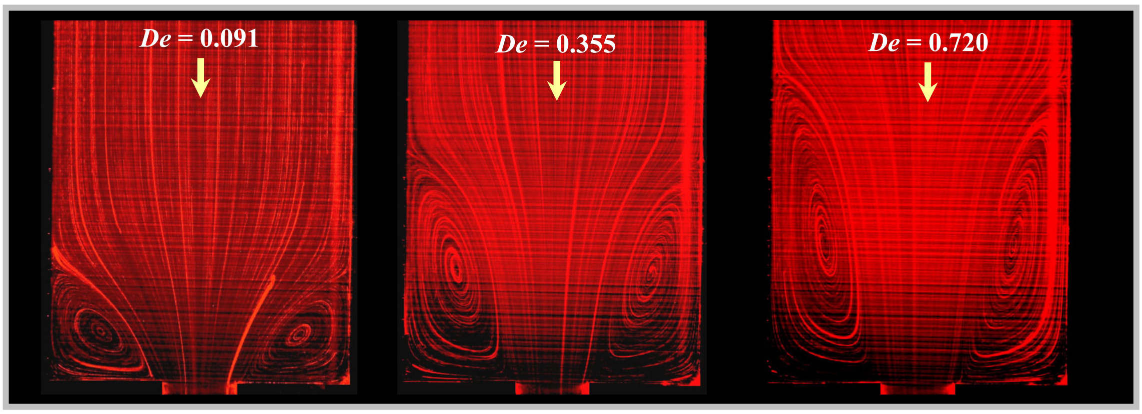

Figure 5. Streaklines in the middle plane as a function of Deborah number for PAA500 fluid under negligible inertia flow conditions.